Genes, Chromosomes and Cancer

WILEY

RESEARCH ARTICLE OPEN ACCESS

Gene Expression Profiles of *AHNAK2*, *DCSTAMP*, *FN1*, and *TERT* Correlate With Mutational Status and Recurrence in Papillary Thyroid Carcinoma

Julia I. Staubitz-Vernazza[1] | Celine Müller[2] | Antonia Heymans[2] | Annekathrin Silvia Nedwed[3] | Mario Schindeldecker[2] | Monika Hartmann[4] | Michael Kloth[2] | Arno Schad[2] | Wilfried Roth[2] | Thomas J. Musholt[1] | Nils Hartmann[2]

[1]Section of Endocrine Surgery, Department of General, Visceral and Transplantation Surgery, University Medical Centre, Johannes Gutenberg University Mainz, Mainz, Germany | [2]Institute of Pathology, University Medical Centre, Johannes Gutenberg University Mainz, Mainz, Germany | [3]Institute for Medical Biometry, Epidemiology and Informatics, University Medical Centre Mainz, Johannes Gutenberg University Mainz, Mainz, Germany | [4]Department of Medicine III, University Medical Centre Mainz, Johannes Gutenberg University Mainz, Mainz, Germany

Correspondence: Nils Hartmann (nils.hartmann@unimedizin-mainz.de)

Received: 23 February 2024 | **Revised:** 11 June 2024 | **Accepted:** 19 June 2024

Funding: This work was supported by the University Medical Centre of the Johannes Gutenberg University Mainz.

Keywords: differentially expressed genes | molecular marker | quantitative RT-PCR | RNA sequencing | thyroid cancer

ABSTRACT

Papillary thyroid carcinoma (PTC), the most common malignancy of follicular cell derivation, is generally associated with good prognosis. Nevertheless, it is important to identify patients with aggressive PTCs and unfavorable outcome. Molecular markers such as $BRAF^{V600E}$ mutation and *TERT* promoter mutations have been proposed for risk stratification. While *TERT* promoter mutations have been frequently associated with aggressive PTCs, the association of $BRAF^{V600E}$ mutation with increased recurrence and mortality is less clear and has been controversially discussed. The aim of the present study was to analyze whether differentially expressed genes can predict $BRAF^{V600E}$ mutations as well as *TERT* promoter mutations in PTCs. RNA sequencing identified a large number of differentially expressed genes between $BRAF^{V600E}$ and $BRAF^{wildtype}$ PTCs. Of those, *AHNAK2*, *DCSTAMP*, and *FN1* could be confirmed in a larger cohort ($n = 91$) to be significantly upregulated in $BRAF^{V600E}$ mutant PTCs using quantitative RT-PCR. Moreover, individual PTC expression values of *DCSTAMP* and *FN1* were able to predict the $BRAF^{V600E}$ mutation status with high sensitivity and specificity. The expression of *TERT* was detected in all PTCs harboring *TERT* promoter mutations and in 19% of PTCs without *TERT* promoter mutations. Tumors with both *TERT* expression and *TERT* promoter mutations were particularly associated with aggressive clinicopathological features and a shorter recurrence-free survival. Altogether, it will be interesting to explore the biological function of *AHNAK2*, *DCSTAMP*, and *FN1* in PTC in more detail. The analysis of their expression patterns could allow the characterization of PTC subtypes and thus enabling a more individualized surgical and medical treatment.

1 | Introduction

Thyroid cancer is the most common endocrine carcinoma. In 2022, it has been estimated that 43 800 new cases of thyroid cancer occurred in the United States [1]. With 31 940 new cases (73%), women are more frequently affected than men [1]. Papillary thyroid carcinoma (PTC) is the most common malignancy of follicular cell derivation in adult and pediatric populations [2, 3]. The

Julia I. Staubitz-Vernazza and Celine Müller contributed equally to this work.

2022 World Health Organization (WHO) classification of thyroid neoplasms describes 13 subtypes of PTC, whereas the former 2017 WHO classification denominated 15 variants of PTC [3, 4]. PTC patients usually show a favorable clinical outcome. However, PTCs can dedifferentiate into more aggressive thyroid cancer characterized by recurrence as well as lymph node and distant metastases [5]. Therefore, it is important to characterize molecular markers that enable an early diagnosis and predict PTC aggressiveness in order to draw conclusions about the individual prognosis. This also allows for an adaptation and individualization of therapy, thereby reducing overdiagnosis and overtreatment. Treatment options for PTC involve surgery, radioactive iodine therapy, thyroid hormone suppression therapy, targeted drug therapy, or chemotherapy [6].

Previous studies of PTC have shown a high frequency of activating somatic alterations of genes encoding effectors in the mitogen-activated protein kinase (MAPK) signaling pathway [7, 8]. Common alterations include point mutations in *BRAF* and the *RAS* genes as well as gene fusions involving *RET* and *NTRK1,-2,-3*. The $BRAF^{V600E}$ mutation is the most common genetic mutation in PTC, which can be identified in 60% of PTCs [7]. Thus, the preoperative discovery of the $BRAF^{V600E}$ mutation in thyroid nodule fine-needle aspirates allows the adaption of the treatment strategy to thyroidectomy with central lymphadenectomy and postoperative radioiodine ablation [9]. Mutations in *NRAS*, *HRAS*, and *KRAS* have been detected in 13% of PTCs, while codon 61 of *NRAS* is the most frequently affected position [7]. In 6% of PTCs, RET rearrangements are detectable, with a variation depending on geographical background and the applied method of assessment [7, 10].

In addition to common driver mutations, *TERT* (*telomerase reverse transcriptase*) promoter mutations also play a role in the pathogenesis of thyroid cancer. Several recent studies show the occurrence of *TERT* promoter mutations in about 7% of PTCs [11–13]. Two *TERT* promoter mutations at chromosome 5 position 1 295 228 C>T and 1 295 250 C>T (referred to as C228T and C250T, respectively) are particularly common. Both mutations create an 11-base nucleotide stretch, which contains a consensus binding site for ETS transcription factors leading to higher telomerase expression [12]. Clinical correlation indicated that *TERT* promoter mutations are associated with a particularly high incidence of radioiodine-refractory disease in patients with PTC distant metastases [14].

While the spectrum of hotspot mutations is rather known in PTCs, less is known about alterations in gene expression. Thus, the aim of this study was the analysis of differentially expressed genes in PTC. We therefore determined gene expression changes using RNA sequencing and quantitative RT-PCR in a cohort of 91 PTCs. Clinical data and mutational status concerning common mutations were known for all PTCs.

2 | Materials and Methods

2.1 | Patient Selection

Tissue specimens were obtained by surgery performed at the Section of Endocrine Surgery, University Medical Centre (UMC) Mainz between 2007 and 2018. Tumor samples were stored as formalin-fixed paraffin-embedded (FFPE) blocks at the Institute of Pathology of the UMC Mainz. Clinicopathological features and mutational status of driver genes of PTC samples were already assessed and recently reported [15]. Tissue samples of 91 PTC patients with tumor cell content ≥30% were included in this study (Table 1). Molecular analyses required the extraction of RNA from PTC tissue samples. RNA was extracted from 4-μm thick FFPE tissue slices using the Maxwell RSC RNA FFPE Kit (Promega, Madison, WI, USA) according to the manufacturer's instructions. Patients showing distant metastasis, recurrence, or occurrence of radioiodine-refractory disease were classified as having an aggressive type of PTC.

2.2 | Detection of Differentially Expressed Genes by RNA Sequencing

Seven PTC tissue samples were selected for RNA sequencing based on high tumor cell content (≥80%), sufficient RNA concentration and quality, and BRAF mutational status. To analyze differentially expressed genes (DEGs) between $BRAF^{V600E}$ ($n = 3$) and $BRAF^{wildtype}$ ($n = 4$) PTCs, RNA sequencing was carried out using the AmpliSeqTM Transcriptome Human Gene Expression Panel (Illumina, San Diego, CA, USA) and the AmpliSeqTM Library PLUS Kit (Illumina, San Diego, CA, USA) according to the manufacturer's instructions. The NextSeq500 System (Illumina, San Diego, CA, USA) was used for library sequencing. Quantification was performed using the Salmon tool [16] and Ensembl genome release GRCh38. Differential expression analysis was carried out with counts in R using the Bioconductor package DESeq2 according to the DESeq2 manual [17] and a DESeq2 tutorial (https://genviz.org/). Genes with adjusted p values <0.05 were considered significant.

The TCGA cohort was downloaded from the GDC data portal [7]. Expression values (fragments per kilobase of transcript per million mapped reads [FPKM]) were downloaded for *ANHAK*, *DCSTAMP*, *FN1*, *TERT*, *GAPDH*, and *ACTB* from 494 PTCs. Of those, 251 cases harbored the *BRAF* mutation p.V600E, and 243 cases had no *BRAF* mutation. FPKM values were compared between $BRAF^{V600E}$ and $BRAF^{wildtype}$ PTCs.

2.3 | Gene Expression Analysis by Quantitative RT-PCR

Only tumor samples with a tumor cell content of ≥30% and a RNA concentration of ≥100 ng/μL were considered for gene expression analysis. For each sample, 1100 ng RNA was transcribed into cDNA using the M-MLV Reverse Transcriptase (Promega, Madison, WI, USA). Quantitative PCR was performed in triplicates using SYBR Green PCR Master Mix (Applied Biosystems, Waltham, MA, USA) on the QuantStudio 5 Real-Time PCR System (Applied Biosystems, Waltham, MA, USA). *ACTB* and *GAPDH* were used as reference genes for normalization based on the cycle threshold value. The following primer pairs were used for PCR amplification: *ACTB fw: 5′-TCCTCTCCCAAGTCCACACA-3′, ACTB rv: 5′-GGCACGAAGGCTCATCATT-3′, AHNAK2 fw: 5′-TAC AGCTCCCAGAGGCAGAT-3′,AHNAK2rv:5′-TGGAGAGGTGC*

TABLE 1 | Clinicopathological features and characteristics of the papillary thyroid carcinoma cohort ($n = 91$) in relation to mutational status. This cohort is part of a larger patient group, and their mutational status has been recently published by Staubitz et al. (n = number, SD = standard deviation).

Parameter	*BRAF*^{V600E}mutant	*RAS* mutant	*RET* rearranged	*NTRK* rearranged	*BRAF*/*RAS*/*RET*/*NTRK* wildtype	Total
Overall cohort, *n* (%)	55 (60.44)	10 (10.99)	9 (9.89)	2 (2.20)	15 (16.48)	91 (100)
Median age, years (±SD)	45 (±14.14)	44 (±17.45)	35 (±17.12)	56 (±1.41)	31 (±17.85)	45 (±15.91)
Sex, *n* (%)						
Female	39 (42.86)	9 (9.89)	5 (5.49)	0 (0)	9 (9.89)	62 (68.13)
Male	16 (17.58)	1 (1.10)	4 (4.40)	2 (2.20)	6 (6.59)	29 (31.87)
Subtype, *n* (%)						
Classical	47 (51.65)	2 (2.20)	8 (8.79)	2 (2.20)	3 (3.30)	62 (68.13)
Follicular	4 (4.40)	8 (8.79)	1 (1.10)	0 (0)	12 (13.19)	25 (27.47)
Oncocytic	2 (2.20)	0 (0)	0 (0)	0 (0)	0 (0)	2 (2.20)
Solid	2 (2.20)	0 (0)	0 (0)	0 (0)	0 (0)	2 (2.20)
Focality, *n* (%)						
Unifocal	37 (40.66)	9 (9.89)	8 (8.79)	2 (2.20)	12 (13.19)	68 (74.73)
Multifocal	18 (19.78)	1 (1.10)	1 (1.10)	0 (0)	3 (3.30)	23 (25.27)
Radioiodine-refractory disease, *n* (%)						
Yes	7 (7.69)	0 (0)	0 (0)	1 (1.10)	1 (1.10)	9 (9.89)
No	48 (52.75)	10 (10.99)	9 (9.89)	1 (1.10)	14 (15.38)	82 (90.11)
Distant metastasis, *n* (%)						
Yes	3 (3.30)	0 (0)	0 (0)	0 (0)	1 (1.10)	4 (4.40)
No	52 (57.14)	10 (10.99)	9 (9.89)	2 (2.20)	14 (15.38)	87 (95.60)
Lymph node metastasis, *n* (%)						
pN1	23 (25.27)	1 (1.10)	6 (6.59)	1 (1.10)	3 (3.30)	34 (37.36)
pN0	27 (29.67)	4 (4.40)	2 (2.20)	0 (0)	8 (8.79)	41 (45.05)
pNx	4 (4.40)	5 (5.49)	1 (1.10)	1 (1.10)	4 (4.40)	15 (16.48)
NA	1 (1.10)	0 (0)	0 (0)	0 (0)	0 (0)	1 (1.10)
Recurrence, *n* (%)						
Yes	9 (9.89)	1 (1.10)	0 (0)	1 (1.10)	2 (2.20)	13 (14.29)
No	46 (50.55)	9 (9.89)	9 (9.89)	1 (1.10)	13 (14.29)	78 (85.71)

AGCTTCAAG-3′, DCSTAMP fw: 5′-GCCTTGCCACTCCAC TAAGT-3′, rv: 5′-GGACTTCCCCTTTGCTGTCA-3′, FN1 fw: 5′-CGGTGGCTGTCAGTCAAAG-3′, FN1 rv: 5′-AAACCTC GGCTTCCTCCATAA-3′, GAPDH fw: 5′-CCCACTCCTCCACC TTTGAC-3′, GAPDH rv: 5′-CCACCACCCTGTTGCTGTAG-3′, TERT fw: 5′-GTCCGAGGTGTCCCTGAGTA-3′, TERT rv: 5′-CAGGGCCTCGTCTTCTACAG-3′. Relative gene expression was calculated with the delta–delta Ct method using the relative expression software tool (REST) [18]. Relative expression values of *AHNAK2*, *DCSTAMP*, and *FN1* were correlated with clinical parameters and PTC histology. Expression of *TERT* was categorized as present or absent. To analyze whether gene expression of *AHNAK2*, *DCSTAMP*, and *FN1* can predict the mutational status, receiver operating characteristic (ROC) curves were generated by stratifying PTCs into low expression (Log2 fold change <0) and into high expression (Log2 fold change >0).

2.4 | Statistical Analysis

All statistical analyses were performed using the R programming language (R Foundation for Statistical Computing, v. 4.1.2, R Core Team 2021, https://www.R-project.org/). Differential expression analysis and statistical testing of the RNA-sequencing data were performed using the "DESeq2" package from Bioconductor according to https://genviz.org/ [17]. Pairwise comparisons between clinical/histological data and relative gene expression levels obtained by quantitative RT-PCR were performed using the Mann–Whitney-*U*-test. Binary logistic regression was used to analyze dependencies between common genetic alterations and the presence of *TERT* expression. The chi-square test or the Fisher's exact test (if the number of patients was <5) were used to determine the significance of differences in clinical parameters between two experimental groups. For survival analyses, it was distinguished between patients with high gene expression values (Log2FC >0) and low gene expression values (Log2FC <0) with respect to *AHNAK2*, *DCSTAMP*, and *FN1*. For *TERT* expression, patients were stratified according to the presence or absence of *TERT* expression. Forty-nine of 91 patients had follow-up times longer than 5 years resulting in a median follow-up time of 63 months. Cox regression was used for recurrence-free survival, and Kaplan–Meier curves were generated to plot recurrence-free survival. Because of multiple testing, *p* values were corrected using the Benjamini–Hochberg procedure to control the false discovery rate [19]. Adjusted *p* values <0.05 were considered significant: $*p < 0.05$, $**p < 0.01$, and $***p < 0.001$. Only adjusted *p* values and 95% confidence intervals (CI) are shown unless stated otherwise. Data were visualized using R and Microsoft Excel (Microsoft Corporation, Redmond, WA, USA).

3 | Results

3.1 | Detection of Differentially Expressed Genes (DEGs) Between $BRAF^{V600E}$ and $BRAF^{wildtype}$ PTCs

Previous studies suggest that $BRAF^{V600E}$-mutant PTCs exhibit a distinct gene expression pattern, the so-called $BRAF^{V600E}$-like signature [7, 20]. Our aim was to identify single genes that are differentially expressed between $BRAF^{V600E}$ and $BRAF^{wildtype}$ PTCs and that may play a role in the tumorigenesis of $BRAF^{V600E}$ PTCs. We therefore selected PTC samples based on high tumor cell content (≥80%), sufficient RNA amount, and the presence or absence of the BRAF mutation p.V600E. Then, we compared transcriptome profiles of $BRAF^{V600E}$-mutated PTCs ($n = 4$) with those of *BRAF/RAS/NTRK*^{wildtype} ($n = 3$) using RNA sequencing. We detected 391 genes that were differentially expressed in $BRAF^{V600E}$ PTCs (Table S1). A total of 174 genes showed significantly increased expression in $BRAF^{V600E}$ tumors, whereas 217 genes were significantly downregulated in those tumors.

One of the significantly upregulated genes was *AHNAK2* (*AHNAK nucleoprotein 2*, $p < 0.001$), which is in accordance with a recent study that reported a positive correlation of *AHNAK2* expression and $BRAF^{V600E}$ PTCs [21]. Furthermore, *DCSTAMP* (*Dendrocyte Expressed Seven Transmembrane Protein*) and *FN1* (*Fibronectin 1*) were significantly higher expressed in $BRAF^{V600E}$ PTCs and two of the top 10 genes with the highest significance ($p < 0.001$, Table S2). All three identified genes showed a more than 6-fold increased mRNA expression in $BRAF^{V600E}$ PTCs compared with $BRAF^{wildtype}$ PTCs (Figure 1A). It is noteworthy that overall expression levels differed among the three genes. While *DCSTAMP* and particularly *AHNAK2* were generally expressed at low levels, *FN1* showed moderate expression levels (Figure 1A).

3.2 | Gene Expression of *AHNAK2*, *DCSTAMP*, and *FN1* Is Significantly Increased in $BRAF^{V600E}$ PTCs Compared With $BRAF^{wildtype}$ PTCs

To validate gene expression of *AHNAK2, DCSTAMP*, and *FN1* in a larger cohort, we established a cohort comprising 91 PTC samples. All cases exhibited sufficient tumor tissue for RNA extraction and a tumor cell content ≥30%. The mutational status of all tumors had been recently determined [15] and included 55 $BRAF^{V600E}$-mutant, 10 *RAS*-mutant, 9 *RET*-rearranged, 2 *NTRK*-rearranged, and 15 *BRAF/RAS/RET/NTRK*-wildtype PTCs. Additional clinicopathologic characteristics of the cohort are summarized in Table 1. Expression of *AHNAK2, DCSTAMP*, and *FN1* was determined using quantitative RT-PCR. All primer pairs and PCR conditions were carefully established and validated. For example, the reference transcripts *ACTB* and *GAPDH* were uniformly expressed in all tumor samples, all primer pairs generated a single PCR product, and except for *TERT*, PCR efficiencies were very close to 100% (range: 99%–104%, Figures S1–S3).

Expression levels of *AHNAK2* and *DCSTAMP* were generally low and could not be detected in every PTC sample. *AHNAK2* expression was found in 68.1% of PTCs (62/91), and *DCSTAMP* expression was detected in 80.2% of PTCs (73/91), while *FN1* expression was found in all analyzed PTCs (91/91). Pairwise comparisons of relative gene expression levels revealed that *AHNAK2* was significantly differentially expressed in $BRAF^{V600E}$ PTCs compared with *BRAF/RAS/RET*-wildtype ($p = 0.031$) and *RET*-rearranged tumors ($p = 0.038$, Figure 2A). Both *DCSTAMP* and *FN1* were differentially expressed in $BRAF^{V600E}$ PTCs at a highly significant level compared with *RAS*-mutant ($p < 0.01$),

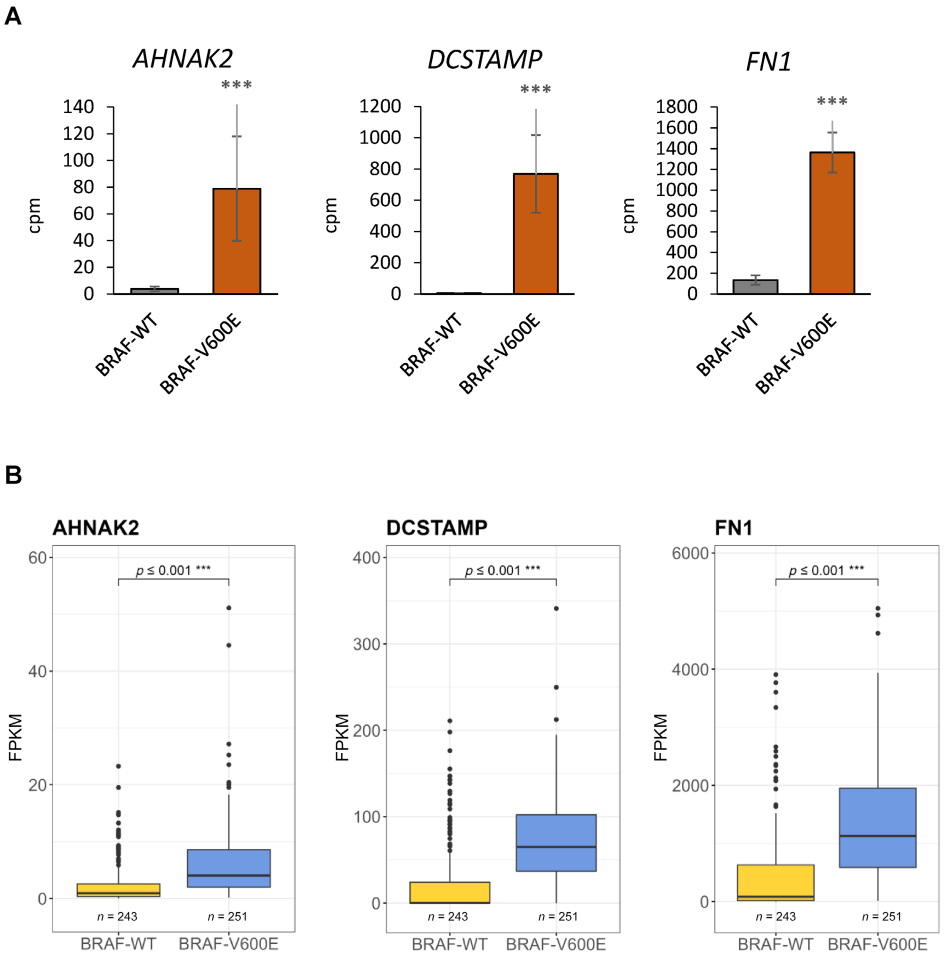

FIGURE 1 | Normalized expression of selected DEGs comparing *BRAF*^{V600E} and *BRAF*^{wildtype} PTCs. (A) Using RNA sequencing, *AHNAK2*, *DCSTAMP*, and *FN1* were significantly upregulated in *BRAF*^{V600E}-mutant PTCs. (B) RNA sequencing data from the TCGA cohort revealed that expression of *AHNAK2*, *DCSTAMP*, and *FN1* was also significantly increased in *BRAF*^{V600E}-mutant PTCs. cpm: counts per million; FPKM: fragments per kilobase of transcript per million mapped reads; *n*: number of PTC samples; WT: wildtype. ***$p < 0.001$.

RET-rearranged ($p < 0.001$), and *BRAF/RAS/RET*-wildtype ($p < 0.001$) tumors. In this regard, *DCSTAMP* and *FN1* showed similar expression patterns with the highest expression in *BRAF*^{V600E} PTCs, intermediate expression in tumors with *RET* rearrangements, and lowest expression in *RAS*-mutant and *BRAF/RAS/RET*-wildtype PTCs (Figure 2A).

In a next step, we analyzed whether expression values of *DCSTAMP* and *FN1* could predict the mutational status concerning *BRAF*^{V600E} or *BRAF*^{wildtype}. A ROC curve was in the upper left corner of the plot and showed a specificity of 95% and a sensitivity of 79% with an area under the curve of 0.957. It shows that both *DCSTAMP* and *FN1* are expressed at low levels in 19 out of 20 *BRAF*^{wildtype} PTCs and that *DCSTAMP* and *FN1*, or at least one of them, are highly expressed in 49 out of 53 *BRAF*^{V600E} PTCs. This indicates that *DCSTAMP* and *FN1* expression allows the discrimination between *BRAF*^{V600E} and *BRAF*^{wildtype} PTCs with high specificity and sensitivity (Figure 2B). Finally, we analyzed expression of *AHNAK2*, *DCTAMP*, and *FN1* in 494 PTCs from the TCGA cohort [7]. In accordance with our observation, all three genes were significantly higher expressed in *BRAF*^{V600E}-mutated tumors compared with *BRAF*^{wildtype} tumors (Figure 1B).

3.3 | *AHNAK2*, *DCSTAMP*, and *FN1* Are Differentially Expressed in Distinct Histological PTC Subtypes

We then assessed whether *AHNAK2*, *DCSTAMP*, and *FN1* expression is associated with clinical outcome or PTC histology. No significant differences in gene expression was found between aggressive and nonaggressive PTCs or between unifocal and multifocal tumors (Figure 3A). *AHNAK2* expression was also not significantly different between classical and follicular subtype ($p = 0.121$), but tended to be slightly increased in classical PTCs. However, the expression of *DCSTAMP* and *FN1* was significantly increased in classical PTCs compared with the follicular subtype (*DCSTAMP*: $p < 0.05$; *FN1*: $p < 0.01$, Figure 3B).

3.4 | TERT Expression and Mutational Status

In the present cohort, 14 (15%) out of 91 PTCs harbored the *TERT* promoter mutation C228T, and no other *TERT* promoter mutation had been identified [15]. Thus, we wanted to determine *TERT* mRNA expression in all PTCs ($n = 91$) using quantitative

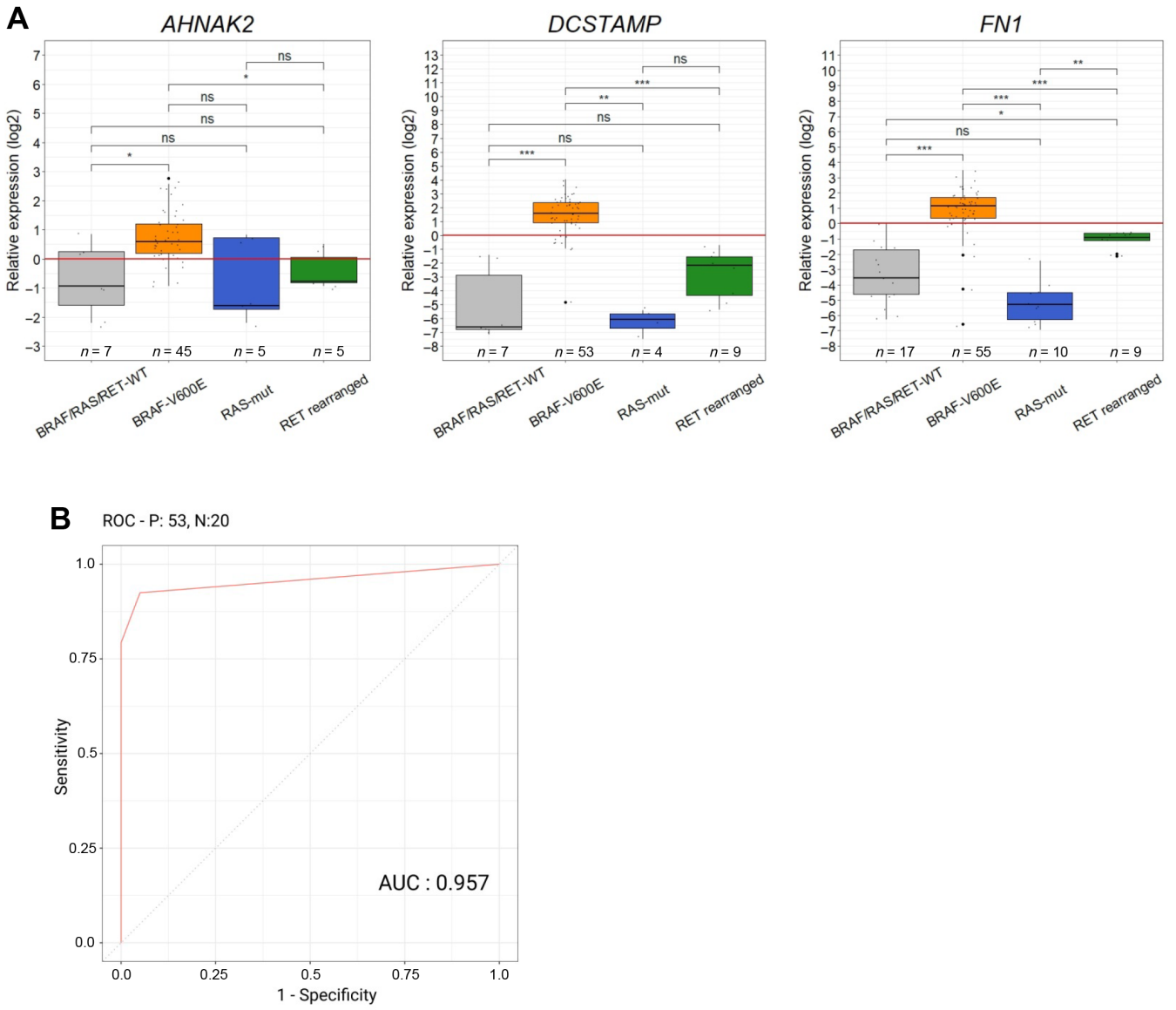

FIGURE 2 | Relative expression of *AHNAK2, DCSTAMP and FN1* in relation to common genetic alterations of PTCs. (A) $BRAF^{V600E}$ PTCs showed increased expression of *AHNAK2, DCSTAMP,* and *FN1*. Expression values were measured by quantitative RT-PCR and normalized to *ACTB* and *GAPDH* expression according to Pfaffl et al. [18]. Each dot represents a relative gene expression value of a single tumor sample, and the slightly larger dots represent outliers. mut: mutant, *n*: number of PTC samples; ns: not significant; WT: wildtype. $*p < 0.05$, $**p < 0.01$, $***p < 0.001$. (B) ROC curve of *DCSTAMP* and *FN1* expression shows a sensitivity of 95% and a specificity of 79% for the presence of $BRAF^{V600E}$ mutations in PTCs. AUC (area under the curve): 0.957, P (positive): $BRAF^{V600E}$-mutant PTCs ($n = 53$), N (negative): $BRAF^{wildype}$ PTCs ($n = 20$).

RT-PCR. The majority of samples showed no detectable *TERT* expression, and when *TERT* expression was detectable, it was very low which prevented a meaningful quantification. Therefore, *TERT* expression was only scored as present or absent based on Ct cycles. Ct values <38 resulted in specific *TERT* amplification suggesting *TERT* expression was present, while Ct values ≥38 resulted in unspecific amplification and thus were considered without *TERT* expression. Altogether, we detected *TERT* expression in 34% of analyzed PTC samples (31/91). The presence of $BRAF^{V600E}$ mutations, *RAS* mutations, or *RET* rearrangements did not significantly correlate with *TERT* expression (Table S3). However, *TERT* expression was found in all PTC samples harboring the *TERT* promoter mutation. In addition, *TERT* expression was also detected in 17 PTCs without *TERT* promoter mutation (Table 2).

3.5 | Impact of TERT Expression and TERT Promoter Status on Clinicopathological Features

In a next step, the clinical impact of both *TERT* mRNA expression and *TERT* promoter status was determined. Therefore, all 91 PTC samples were distributed into three groups based on their *TERT* promoter and *TERT* expression status. The first group consisted of *TERT* expression-positive PTCs and harboring the *TERT* promoter mutation ($TERT^{exp(+)}/pTERT^{mut}$). The second group comprised

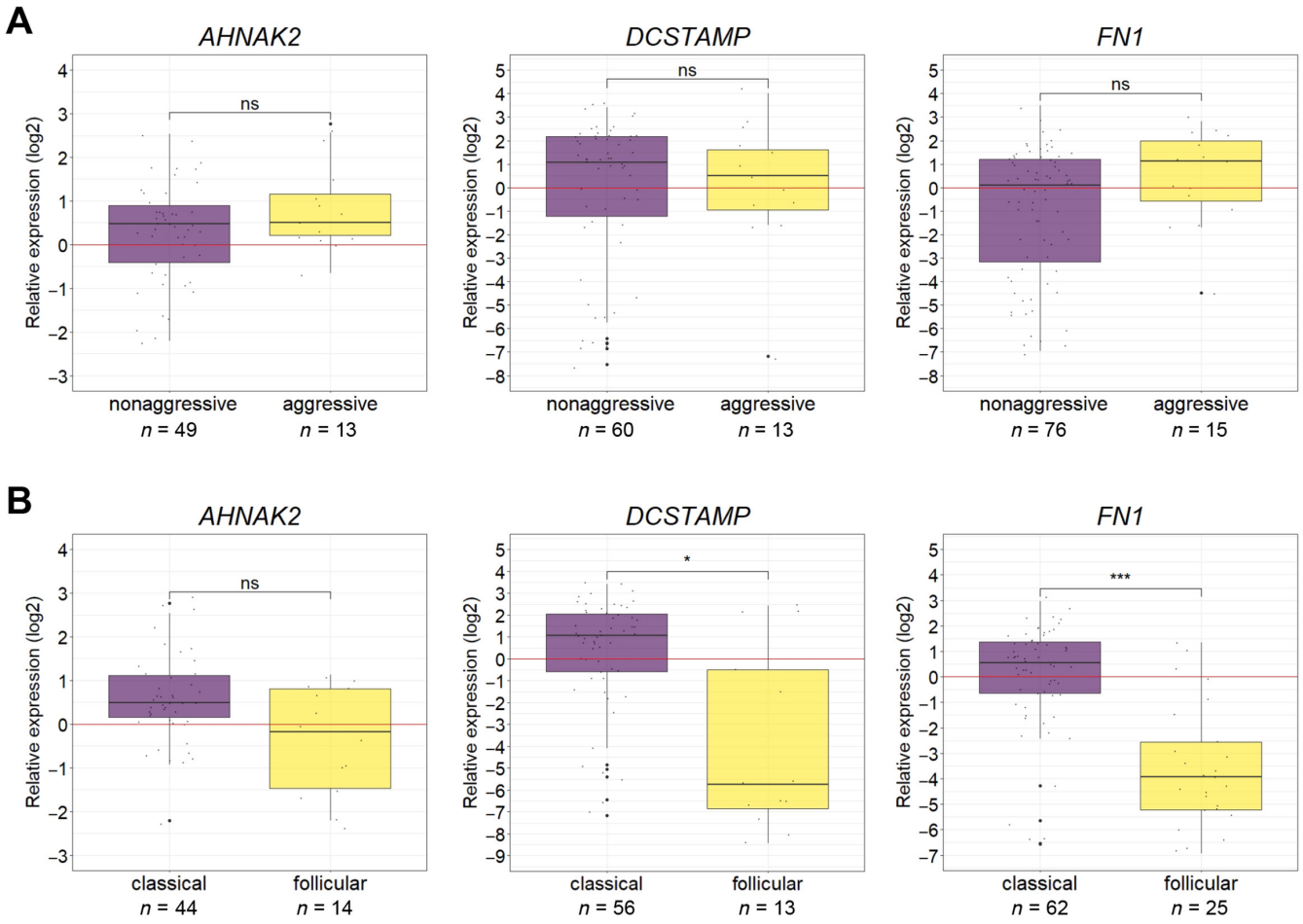

FIGURE 3 | Relative expression of *AHNAK2*, *DCSTAMP*, and *FN1* in relation to clinicopathological and histological characteristics. (A) Patients showing distant metastasis, recurrence, or radioiodine-refractory disease were classified as having an aggressive type of PTC. There was no significant difference in *AHNAK2*, *DCSTAMP*, and *FN1* expression between aggressive and nonaggressive PTCs. (B) *DCSTAMP* and *FN1* showed differential expression in classical PTCs than in follicular subtypes. *AHNAK2* expression was slightly but not significantly increased in classical PTCs. Expression values were determined by quantitative RT-PCR and normalized to *ACTB* and *GAPDH* expression. The oncocytic and solid variants were neglected due to their low sample number. *n*: number of PTC samples, ns: not significant. $*p < 0.05$, $***p < 0.001$.

TABLE 2 | Overview about PTCs with *TERT* expression in relation to their *TERT* promoter status (*n*: number of PTC samples; %: percentage of PTC samples in relation to all 91 analyzed samples).

	***TERT* promoter mutant, *n* (%)**	***TERT* promoter wildtype, *n* (%)**
TERT expression positive (+)	14 (15.4%)	17 (18.7%)
TERT expression negative (–)	0 (0%)	60 (65.9%)

TERT expression-positive tumors without *TERT* promoter mutation ($TERT^{exp(+)}/pTERT^{wildtype}$). The third group consisted of *TERT* expression-negative PTC samples in absence of *TERT* promoter mutation ($TERT^{exp(-)}/pTERT^{wildtype}$). Pairwise comparisons revealed no significant differences regarding age, sex, PTC subtype, tumor focality, and affected lymph nodes between all three groups (Table 3). It was found that patients with $TERT^{exp(+)}/pTERT^{mut}$ tumors showed a significantly higher occurrence of radioiodine-refractory disease and recurrence rate. Distant metastases were exclusively observed in PTCs with $TERT^{exp(+)}/pTERT^{mut}$. Moreover, patients with tumors expressing *TERT* but without promoter mutation ($TERT^{exp(+)}/pTERT^{wildtype}$) did not show a significantly higher incidence of radioiodine-refractory disease, distant metastasis, and recurrence (Table 3).

3.6 | TERT Expression and TERT Promoter Mutation Are Associated With Shorter Recurrence-Free Survival

Finally, the prognostic value of *AHNAK2*, *DCSTAMP*, *FN1*, and *TERT* expression for recurrence-free survival was investigated. Therefore, all PTC samples were stratified into a low and a high expression group for *AHNAK2*, *DCSTAMP*,

TABLE 3 | Clinicopathological features and characteristics of the papillary thyroid carcinoma cohort ($n = 91$) in relation to *TERT* expression and *TERT* promoter status.

	Group 1 $TERT^{exp(+)}/pTERT^{mut}$	Group 2 $TERT^{exp(+)}/pTERT^{wildtype}$	Group 3 $TERT^{exp(-)}/pTERT^{wildtype}$	Total	$p_{1vs.2}$	$p_{1vs.3}$	$p_{2vs.3}$
Age, *n* (%)					0.210	0.088	1
<55	6 (42.86)	13 (76.47)	47 (78.33)	66 (72.53)			
>55	8 (57.14)	4 (23.53)	13 (21.67)	25 (27.47)			
Total	14 (100)	17 (100)	60 (100)	91 (100)			
Sex, *n* (%)					0.694	0.860	0.947
Female	8 (57.14)	13 (76.47)	41 (68.33)	62 (68.13)			
Male	6 (42.86)	4 (23.53)	19 (31.67)	29 (31.87)			
Total	14 (100)	17 (100)	60 (100)	91 (100)			
Subtype, *n* (%)					0.420	0.215	1
Classical	12 (85.71)	12 (70.59)	38 (63.33)	62 (68.13)			
Follicular	1 (7.14)	5 (29.41)	19 (31.67)	25 (27.47)			
Other*	1 (7.14)	0 (0)	3 (5)	4 (4.40)			
Total	14 (100)	17 (100)	60 (100)	91 (100)			
Focality, *n* (%)					0.478	1	0.173
Unifocal	11 (78.57)	9 (52.94)	48 (80.0)	68 (74.73)			
Multifocal	3 (21.43)	8 (47.06)	12 (20.0)	23 (25.27)			
Total	14 (100)	17 (100)	60 (100)	91 (100)			
Radioiodine-refractory disease, *n* (%)					**0.003**	**<0.001**	1
Yes	8 (57.14)	0 (0)	1 (1.67)	9 (9.98)			
No	6 (42.86)	17 (100)	59 (98.33)	82 (90.11)			
Total	14 (100)	17 (100)	60 (100)	91 (100)			
Distant metastasis, *n* (%)					0.118	**0.006**	—
Yes	4 (28.57)	0 (0)	0 (0)	4 (4.40)			
No	10 (71.43)	17 (100)	60 (100)	87 (95.60)			
Total	14 (100)	17 (100)	60 (100)	91 (100)			

(Continues)

TABLE 3 | (Continued)

	Group 1	Group 2	Group 3		$p_{1vs.2}$	$p_{1vs.3}$	$p_{2vs.3}$
	$TERT^{exp(+)}/pTERT^{mut}$	$TERT^{exp(+)}/pTERT^{wildtype}$	$TERT^{exp(-)}/pTERT^{wildtype}$	Total			
Lymph node metastasis, *n* (%)					0.976	0.694	0.210
Yes	6 (42.86)	10 (58.82)	18 (30.0)	34 (37.36)			
No	5 (35.71)	5 (29.41)	31 (51.67)	41 (45.05)			
NA*	3 (21.43)	2 (11.76)	11 (18.33)	16 (17.58)			
Total	14 (100)	17 (100)	60 (100)	91 (100)			
Recurrence, *n* (%)					**0.035**	**<0.001**	0.420
Yes	9 (64.29)	2 (11.76)	2 (3.33)	13 (14.29)			
No	5 (35.71)	15 (88.24)	58 (96.67)	78 (85.71)			
Total	14 (100)	17 (100)	60 (100)	91 (100)			

Note: Significant *p*-values are shown in bold.

and *FN1*, respectively. Regarding *TERT*, PTCs were stratified based on the presence or absence of *TERT* expression and the *TERT* expressing group was further subdivided into PTCs with or without *TERT* promotor mutation. Kaplan–Meier analyses revealed no significant differences in recurrence-free survival between high or low expression of *AHNAK2*, *DCSTAMP*, and *FN1* (Figure 4A–C). In contrast, patients with *TERT* expressing PTCs had significantly shorter recurrence-free survival than patients without *TERT* expression ($p < 0.001$, Figure 4D). To further assess the prognostic role of *TERT*, we analyzed the impact of the *TERT* promoter status. Patients with both *TERT* expression and *TERT* promoter mutation ($TERT^{exp(+)}/pTERT^{mut}$) also showed decreased recurrence-free survival ($p < 0.001$, Figure 4E). Interestingly, patients with *TERT* expression but without *TERT* promoter mutation ($TERT^{exp(+)}/pTERT^{wildtype}$) were by tendency associated with decreased recurrence-free survival, but the effect was not significant ($p = 0.124$, Figure 4F).

4 | Discussion

In this study, we used a combined approach consisting of RNA sequencing and quantitative RT-PCR to identify genes that show significant differences in mRNA levels between PTCs with different driver mutations. Among 91 PTCs evaluated in this study, the $BRAF^{V600E}$ mutation was detected in 60% of all cases, *RAS* mutations in 11%, *RET* rearrangements in 10%, *NTRK* rearrangements in 2%, and *TERT* promoter mutation in 15%. In that way, the frequencies of driver mutations in the present cohort resembles the frequencies found in the 496 PTCs of the TCGA study (*BRAF*-mutant: 60%, *RAS*-mutant: 13%, *RET*-rearranged: 6%, *NTRK*-rearranged: 2%, and *pTERT*-mutant: 9%) [7]. Although *BRAF* and *RAS* mutations as well as *RET* and *NTRK* fusions affect MAPK signaling, differences have been reported concerning signaling intensity. For example, it was shown that $BRAF^{V600E}$ tumors do not respond to the negative feedback from ERK to RAF, as $BRAF^{V600E}$ signals as a monomer [22], which results in high MAPK-signaling. In contrast, *RAS*-mutant tumors respond to ERK feedback via RAF dimers, which results in lower MAPK-signaling. Furthermore, *RAS*-mutant PTCs additionally activate PI3K/AKT-signaling, as shown by increased pAKT levels in those tumors [7]. This led to the discovery of distinct gene expression patterns in PTC depending on the mutational status. The authors of the TCGA study have identified a $BRAF^{V600E}$-like gene expression pattern and a *RAS*-like pattern [7]. Yoo et al. proposed a third gene expression pattern in PTC, which they named *non-BRAF, non-RAS*-like gene expression pattern [23]. While distinct gene expression patterns allow the discrimination of PTCs into $BRAF^{V600E}$-like or *RAS*-like, little is known about the expression of single genes that might contribute to these patterns [24].

We identified three genes, *AHNAK2*, *DCSTAMP*, and *FN1*, to be highly upregulated in $BRAF^{V600E}$-mutant PTCs. The gene *AHNAK2* (*AHNAK Nucleoprotein 2*), which encodes a large nucleoprotein with a PDZ domain, was previously reported to be overexpressed in various cancers including bladder cancer, lung cancer, cellular cell renal cell carcinoma, and thyroid cancer [25–28]. *AHNAK2* expression has been suggested

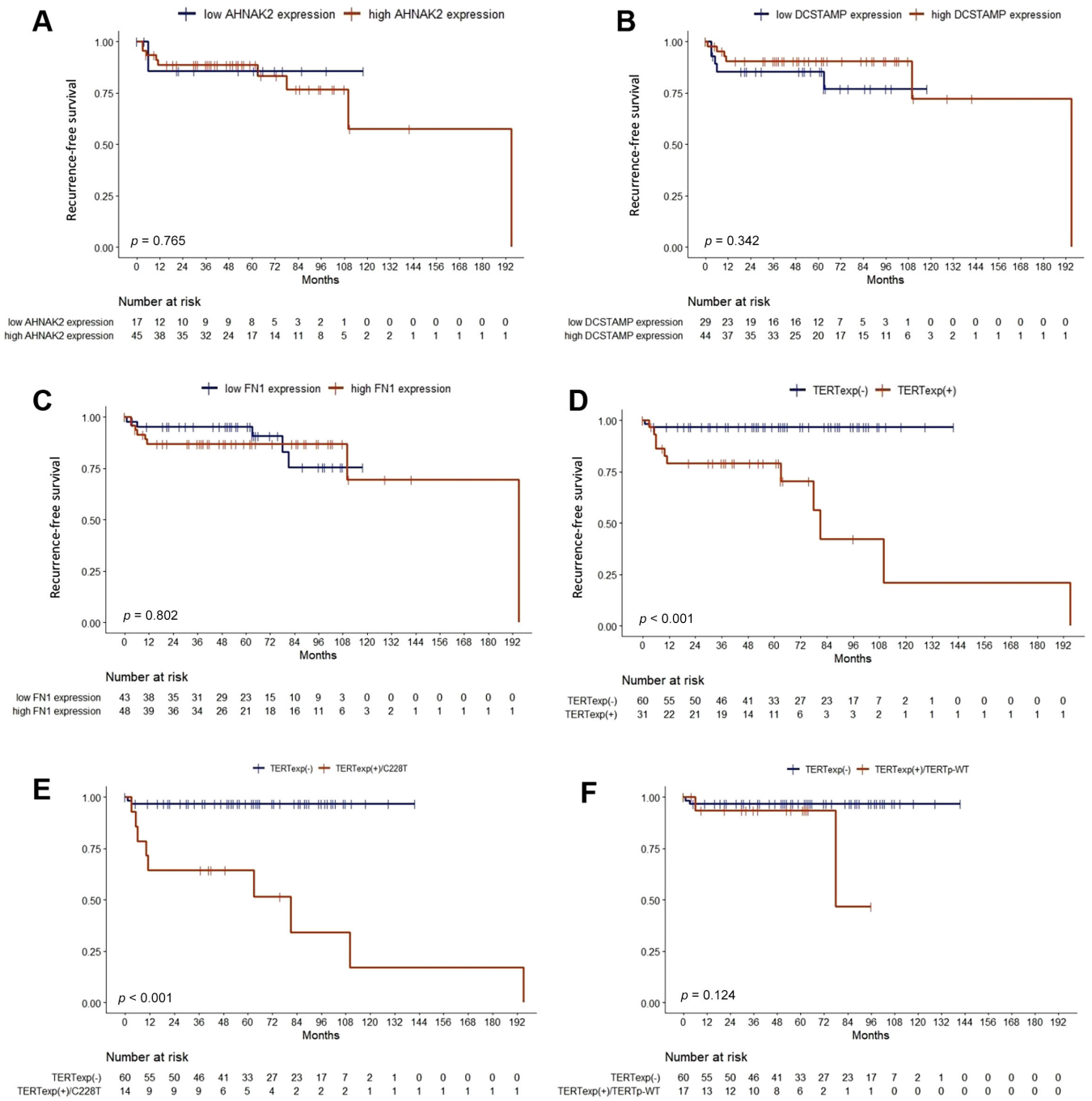

FIGURE 4 | Kaplan–Meier curves of recurrence-free survival. Recurrence-free survival is shown depending on low or high *AHNAK2* expression (A), *DCSTAMP* expression (B), *FN1* expression (C), and on absence or presence of *TERT* expression (D). In addition, recurrence-free survival is shown depending on absent *TERT* expression and present *TERT* expression plus *TERT* promoter mutation (E) as well as depending on absent *TERT* expression and present *TERT* expression without *TERT* promoter mutation (F).

to promote PI3K/AKT signaling pathway [29], Wnt/β-catenin pathway [30], and NF-κB activity [31]. *AHNAK2* was also associated with immune cell infiltration in PTC [26]. Furthermore, altered *AHNAK2* expression levels were associated with aggressive clinicopathological features. Recent studies have shown that *AHNAK2* was particularly upregulated in metastatic and advanced thyroid carcinomas as well as in *BRAF*-mutant tumors [21, 26]. Thus, it is not surprising that downregulation of *AHNAK2* in thyroid cancer cells restricted proliferation, metastasis, and epithelial-mesenchymal transition [30]. In this study, PTC patients did not show significant differences in *AHNAK2* expression between clinically aggressive and nonaggressive PTCs. However, the high expression of *AHNAK2* in *BRAF*-mutant tumors is in accordance with other reports [21, 26].

The second gene we found to be highly upregulated in $BRAF^{V600E}$ PTCs was *DCSTAMP* (*Dendrocyte Expressed Seven Transmembrane Protein*), also known as *DC-STAMP* or *TM7SF4*. DCSTAMP is an approximately 50 kDa glycoprotein with seven transmembrane segments. It is mainly expressed on

the surface of dendritic cells and monocytes as well as on osteoclasts and their progenitors. It is involved in the regulation of immune responses, antigen processing, and cell differentiation [32–34]. Moreover, it has been suggested that downregulation of *DCSTAMP* leads to inhibition of proliferation and metastasis in lung cancer and that *DCSTAMP* plays an important role in cell cycle regulation in breast cancer [32, 35]. As in the present study, it has been also reported that *DCSTAMP* shows higher expression in $BRAF^{V600E}$ PTCs compared with $BRAF^{wildtype}$ PTCs [33, 36, 37]. In contrast to the present study, a recent report found that upregulation of the DCSTAMP protein was associated with unfavorable outcomes in PTC [37]. These results suggest that DCSTAMP could be a potential therapeutic target in $BRAF^{V600E}$ PTCs; however, the exact role of DCSTAMP in PTC remains unclear.

FN1 (*fibronectin 1*) was the third gene found in the present study, which was highly expressed in $BRAF^{V600E}$ PTCs. *FN1* encodes for fibronectin, a high-molecular weight glycoprotein of the extracellular matrix. Fibronectin has been considered as one of the biomarkers of epithelial-mesenchymal transition (EMT) providing cancer cells to migrate from the primary tumor and to invade surrounding and distant tissues. It has been shown that increased *FN1* expression in PTC correlates with lymph node metastasis and with more aggressive PTCs [38, 39]. Sponziello et al. demonstrated that *FN1* expression was higher in *BRAF*-mutant tumors and that treating the *BRAF*-mutant PTC cell line BCPAP with the BRAF inhibitor Vemurafenib reduced *FN1* expression suggesting a link between *FN1* expression and BRAF-signaling. Although there was no significant difference in *FN1* expression between samples of the aggressive and nonaggressive PTC group in this study, *FN1* tended to be slightly increased in patients with distant metastasis, recurrence, and/or iodine-refractory disease.

Although *AHNAK2*, *DCSTAMP*, and *FN1* encode for functionally diverse proteins that are involved in different pathways, their expression highly correlates in PTC depending on the mutational status of *BRAF*. In particular, the expression level of *DCSTAMP* and *FN1* allows discriminating between $BRAF^{V600E}$ and $BRAF^{wildtype}$ PTCs with high sensitivity and specificity. Furthermore, expression of *AHNAK2*, *DCSTAMP*, and *FN1* was also significantly increased in $BRAF^{V600E}$ PTCs from the TCGA cohort [7]. In that way the TCGA data confirmed the present findings. Expression of *DCSTAMP* and *FN1* was also increased in classical PTCs compared with the follicular subtype. One explanation for this effect could be the unequal distribution of $BRAF^{V600E}$ mutations among the subtypes. According to our observation, 68% of classical PTCs harbor a $BRAF^{V600E}$ mutation, whereas only 30% of follicular PTCs show a $BRAF^{V600E}$ mutation [15]. As mentioned above, several studies reported that high expression of *AHNAK2*, *DCSTAMP*, and *FN1* correlates with aggressive clinicopathological features of PTCs [21, 26, 37–39]. We could not find this correlation in the present study. This might be attributed to the low number of PTC patients showing aggressive features. Another reason could be that other studies also found a correlation between $BRAF^{V600E}$-mutant and aggressive PTCs. In our recent study, we did not observe a significant correlation between $BRAF^{V600E}$ mutational status and aggressive features [15], which is consistent with the lack of correlation between *AHNAK2*, *DCSTAMP*, and *FN1* expression and aggressiveness among the present cohort.

The pattern of *TERT* mRNA expression was entirely different from the expression of *AHNAK2*, *DCSTAMP*, and *FN1*. There was no correlation between *TERT* expression and the mutational status regarding common alterations in *BRAF*, *RAS*, *RET*, or *NTRK1*. Instead, *TERT* expression was detected in all PTC samples harboring the *TERT* promoter mutation C228T. This substitution has been previously described to create an 11-base nucleotide stretch 5′-CCCCTTCCGGG-3′, which generates a new consensus binding site for ETS transcription factors leading to higher telomerase expression [11, 12, 40]. Moreover, *TERT* expression was found in 17 PTCs (19%, total $n = 91$), which harbored no *TERT* promoter mutation. This can be explained by possible other mechanisms for initiation and promoting *TERT* expression. For instance, amplification of the proto-oncogene *MYC* has been shown to activate *TERT* promoter in a mutation independent way [13]. *TERT* copy number gain was associated with *TERT* upregulation in breast cancer [41]. Promoter methylation has been also reported to be able to increase *TERT* expression [42]. We did not analyze for the occurrence of these mechanisms. However, we found that PTCs with *TERT* expression and without *TERT* promoter mutation showed no significant correlation with aggressive clinicopathological features, whereas PTCs with both *TERT* expression and *TERT* promoter mutation significantly correlated with aggressive clinicopathological features. The underlying mechanisms for this discrepancy are not clear.

In summary, the identified genes *AHNAK2*, *DCSTAMP*, and *FN1* are crucial factors among the $BRAF^{V600E}$-like gene expression pattern. They are not only upregulated in *BRAF*-mutant PTCs but their expression levels allow rather specific prediction about the presence or absence of the $BRAF^{V600E}$ mutation in each individual PTC of the current cohort. Little is known about the regulation of their expression and whether high MAPK-signaling in $BRAF^{V600E}$-mutant tumors may directly activate their expression. In general, it will be interesting to investigate the role and function of *AHNAK2*, *DCSTAMP*, and *FN1* in PTC. The presence of *TERT* promoter mutations have already been described to correlate with aggressive PTCs and unfavorable prognosis [12, 40]. In the present study, all PTCs harboring the *TERT* promoter mutation showed detectable *TERT* mRNA expression and were significantly associated with aggressive clinicopathological features. It is noteworthy to mention that PTCs with detectable *TERT* expression but without *TERT* promoter mutation showed no significant association with aggressive clinicopathological features. In future, it will be worth to study those PTCs in more detail and to find possible mechanisms for this observation.

Author Contributions

All authors contributed to the study conception and design. Material preparation, data collection, and analysis were performed by Julia I. Staubitz-Vernazza, Celine Müller, and Antonia Heymans. The first draft of the manuscript was written by Nils Hartmann. All authors read and approved the final manuscript.

Acknowledgments

We thank Doris Dreis and Nadine Dexheimer for excellent technical assistance. Open Access funding enabled and organized by Projekt DEAL.

Ethics Statement

All procedures performed in this study involving human participants were in accordance with the ethical standards of the institutional research committee and with the 1964 Helsinki Declaration and its later amendments.

Conflicts of Interest

The authors declare no conflicts of interest.

Data Availability Statement

Data will be available on reasonable request.

References

1. R. L. Siegel, K. D. Miller, H. E. Fuchs, and A. Jemal, "Cancer Statistics, 2022," *CA: A Cancer Journal for Clinicians* 72 (2022): 7–33.

2. C. M. Kitahara and J. A. Sosa, "Understanding the Ever-Changing Incidence of Thyroid Cancer," *Nature Reviews. Endocrinology* 16 (2020): 617–618.

3. Z. W. Baloch, S. L. Asa, J. A. Barletta, et al., "Overview of the 2022 WHO Classification of Thyroid Neoplasms," *Endocrine Pathology* 33 (2022): 27–63.

4. R. V. Lloyd, R. Y. Osamura, G. Klöppel, and J. Rosai, *WHO Classification of Tumours of Endocrine Organs* (Lyon: IARC, 2017).

5. P. E. Voutilainen, M. M. Multanen, A. K. Leppaniemi, C. H. Haglund, R. K. Haapiainen, and K. O. Franssila, "Prognosis After Lymph Node Recurrence in Papillary Thyroid Carcinoma Depends on Age," *Thyroid* 11 (2001): 953–957.

6. J. A. Fagin and S. A. Wells, "Biologic and Clinical Perspectives on Thyroid Cancer," *New England Journal of Medicine* 375 (2016): 1054–1067.

7. Cancer Genome Atlas Research Network, "Integrated Genomic Characterization of Papillary Thyroid Carcinoma," *Cell* 159 (2014): 676–690.

8. E. T. Kimura, M. N. Nikiforova, Z. Zhu, J. A. Knauf, Y. E. Nikiforov, and J. A. Fagin, "High Prevalence of BRAF Mutations in Thyroid Cancer: Genetic Evidence for Constitutive Activation of the RET/PTC-RAS-BRAF Signaling Pathway in Papillary Thyroid Carcinoma," *Cancer Research* 63 (2003): 1454–1457.

9. T. J. Musholt, C. Fottner, M. M. Weber, et al., "Detection of Papillary Thyroid Carcinoma by Analysis of BRAF and RET/PTC1 Mutations in Fine-Needle Aspiration Biopsies of Thyroid Nodules," *World Journal of Surgery* 34 (2010): 2595–2603.

10. M. N. Nikiforova, C. M. Caudill, P. Biddinger, and Y. E. Nikiforov, "Prevalence of RET/PTC Rearrangements in Hashimoto's Thyroiditis and Papillary Thyroid Carcinomas," *International Journal of Surgical Pathology* 10 (2002): 15–22.

11. F. Panebianco, A. V. Nikitski, M. N. Nikiforova, and Y. E. Nikiforov, "Spectrum of TERT Promoter Mutations and Mechanisms of Activation in Thyroid Cancer," *Cancer Medicine* 8 (2019): 5831–5839.

12. X. Liu, J. Bishop, Y. Shan, et al., "Highly Prevalent TERT Promoter Mutations in Aggressive Thyroid Cancers," *Endocrine-Related Cancer* 20 (2013): 603–610.

13. R. Y. Liu, T. Zhang, G. W. Zhu, and M. Z. Xing, "Regulation of Mutant TERT by BRAF V600E/MAP Kinase Pathway Through FOS/GABP in Human Cancer," *Nature Communications* 9 (2018): 579.

14. X. Yang, J. Li, X. Li, et al., "TERT Promoter Mutation Predicts Radioiodine-Refractory Character in Distant Metastatic Differentiated Thyroid Cancer," *Journal of Nuclear Medicine* 58 (2017): 258–265.

15. J. I. Staubitz, C. Muller, A. Heymans, et al., "Approach to Risk Stratification for Papillary Thyroid Carcinoma Based on Molecular Profiling: Institutional Analysis," *BJS Open* 7 (2023): zrad029.

16. R. Patro, G. Duggal, M. I. Love, R. A. Irizarry, and C. Kingsford, "Salmon Provides Fast and Bias-Aware Quantification of Transcript Expression," *Nature Methods* 14 (2017): 417–419.

17. M. I. Love, W. Huber, and S. Anders, "Moderated Estimation of Fold Change and Dispersion for RNA-Seq Data With DESeq2," *Genome Biology* 15 (2014): 550.

18. M. W. Pfaffl, "A New Mathematical Model for Relative Quantification in Real-Time RT-PCR," *Nucleic Acids Research* 29 (2001): e45.

19. Y. Benjamini and J. Hochberg, "Controlling the False Discovery Rate: A Practical and Powerful Approach to Multiple Testing," *Journal of the Royal Statistical Society: Series B (Methodological)* 57 (1995): 289–300.

20. S. K. Yoo, Y. S. Song, E. K. Lee, et al., "Integrative Analysis of Genomic and Transcriptomic Characteristics Associated With Progression of Aggressive Thyroid Cancer," *Nature Communications* 10 (2019): 2764.

21. Z. Xie, Y. Lun, X. Li, et al., "Bioinformatics Analysis of the Clinical Value and Potential Mechanisms of AHNAK2 in Papillary Thyroid Carcinoma," *Aging (Albany NY)* 12 (2020): 18163–18180.

22. C. A. Pratilas, B. S. Taylor, Q. Ye, et al., "(V600E)BRAF Is Associated With Disabled Feedback Inhibition of RAF-MEK Signaling and Elevated Transcriptional Output of the Pathway," *Proceedings of the National Academy of Sciences of the United States of America* 106 (2009): 4519–4524.

23. S. K. Yoo, S. Lee, S. J. Kim, et al., "Comprehensive Analysis of the Transcriptional and Mutational Landscape of Follicular and Papillary Thyroid Cancers," *PLoS Genetics* 12 (2016): e1006239.

24. Y. Nagayama and H. Mishima, "Heterogenous Nature of Gene Expression Patterns in BRAF-Like Papillary Thyroid Carcinomas With BRAF(V600E)," *Endocrine* 66 (2019): 607–613.

25. D. Koguchi, K. Matsumoto, Y. Shimizu, et al., "Prognostic Impact of AHNAK2 Expression in Patients Treated With Radical Cystectomy," *Cancers (Basel)* 13 (2021): 1748.

26. L. Zheng, S. Li, X. Zheng, R. Guo, and W. Qu, "AHNAK2 Is a Novel Prognostic Marker and Correlates With Immune Infiltration in Papillary Thyroid Cancer: Evidence From Integrated Analysis," *International Immunopharmacology* 90 (2021): 107185.

27. M. Wang, X. Li, J. Zhang, et al., "AHNAK2 Is a Novel Prognostic Marker and Oncogenic Protein for Clear Cell Renal Cell Carcinoma," *Theranostics* 7 (2017): 1100–1113.

28. M. Zheng, J. Liu, T. Bian, et al., "Correlation Between Prognostic Indicator AHNAK2 and Immune Infiltrates in Lung Adenocarcinoma," *International Immunopharmacology* 90 (2021): 107134.

29. M. Xu, J. Wen, Q. Xu, et al., "AHNAK2 Promotes the Progression of Differentiated Thyroid Cancer Through PI3K/AKT Signaling Pathway," *Current Cancer Drug Targets* 24, no. 2 (2024): 220–229.

30. Q. Y. Lin, Q. L. Qi, S. Hou, et al., "Silencing of AHNAK2 Restricts Thyroid Carcinoma Progression by Inhibiting the Wnt/Beta-Catenin Pathway," *Neoplasma* 68 (2021): 1063–1071.

31. R. Ye, D. Liu, H. Guan, et al., "AHNAK2 Promotes Thyroid Carcinoma Progression by Activating the NF-KappaB Pathway," *Life Sciences* 286 (2021): 120032.

32. X. Yang, X. Song, X. Wang, X. Liu, and Z. Peng, "Downregulation of TM7SF4 Inhibits Cell Proliferation and Metastasis of A549 Cells Through Regulating the PI3K/AKT/mTOR Signaling Pathway," *Molecular Medicine Reports* 16 (2017): 6122–6127.

33. T. J. Giordano, R. Kuick, D. G. Thomas, et al., "Molecular Classification of Papillary Thyroid Carcinoma: Distinct BRAF, RAS, and RET/PTC Mutation-Specific Gene Expression Profiles Discovered by DNA Microarray Analysis," *Oncogene* 24 (2005): 6646–6656.

34. Y. Sawatani, T. Miyamoto, S. Nagai, et al., "The Role of DC-STAMP in Maintenance of Immune Tolerance Through Regulation of Dendritic Cell Function," *International Immunology* 20 (2008): 1259–1268.

35. X. X. Zeng, T. J. Chu, J. Y. Yuan, et al., "Transmembrane 7 Superfamily Member 4 Regulates Cell Cycle Progression in Breast Cancer Cells," *European Review for Medical and Pharmacological Sciences* 19 (2015): 4353–4361.

36. D. Rusinek, M. Swierniak, E. Chmielik, et al., "BRAFV600E-Associated Gene Expression Profile: Early Changes in the Transcriptome, Based on a Transgenic Mouse Model of Papillary Thyroid Carcinoma," *PLoS One* 10 (2015): e0143688.

37. J. J. Lee, Y. C. Hsu, W. C. Huang, and S. P. Cheng, "Upregulation of Dendrocyte-Expressed Seven Transmembrane Protein Is Associated With Unfavorable Outcomes in Differentiated Thyroid Cancer," *Endocrine* 81 (2023): 513–520.

38. M. Sponziello, F. Rosignolo, M. Celano, et al., "Fibronectin-1 Expression Is Increased in Aggressive Thyroid Cancer and Favors the Migration and Invasion of Cancer Cells," *Molecular and Cellular Endocrinology* 431 (2016): 123–132.

39. S. Xia, C. Wang, E. L. Postma, Y. Yang, X. Ni, and W. Zhan, "Fibronectin 1 Promotes Migration and Invasion of Papillary Thyroid Cancer and Predicts Papillary Thyroid Cancer Lymph Node Metastasis," *Oncotargets and Therapy* 10 (2017): 1743–1755.

40. A. Tanaka, M. Matsuse, V. Saenko, et al., "TERT mRNA Expression as a Novel Prognostic Marker in Papillary Thyroid Carcinomas," *Thyroid* 29 (2019): 1105–1114.

41. M. Gay-Bellile, L. Veronese, P. Combes, et al., "TERT Promoter Status and Gene Copy Number Gains: Effect on TERT Expression and Association With Prognosis in Breast Cancer," *Oncotarget* 8 (2017): 77540–77551.

42. L. Losi, L. Botticelli, L. Garagnani, et al., "TERT Promoter Methylation and Protein Expression as Predictive Biomarkers for Recurrence Risk in Patients With Serous Borderline Ovarian Tumours," *Pathology* 53 (2021): 187–192.

Supporting Information

Additional supporting information can be found online in the Supporting Information section.